Physics Letters B 773 (2017) 544–552

Contents lists available at ScienceDirect

Physics Letters B

www.elsevier.com/locate/physletb

Bilepton signatures at the LHC

Gennaro Corcella [a], Claudio Corianò [b,*], Antonio Costantini [b], Paul H. Frampton [b]

[a] INFN, Laboratori Nazionali di Frascati, Via E. Fermi 40, 00044, Frascati (RM), Italy
[b] Dipartimento di Matematica e Fisica "Ennio De Giorgi", Università del Salento and INFN-Lecce, Via Arnesano, 73100 Lecce, Italy

ARTICLE INFO

Article history:
Received 8 July 2017
Received in revised form 8 September 2017
Accepted 8 September 2017
Available online 12 September 2017
Editor: A. Ringwald

ABSTRACT

We discuss the main signatures of the Bilepton Model at the Large Hadron Collider, focusing on its gauge boson sector. The model is characterised by five additional gauge bosons, four charged and one neutral, beyond those of the Standard Model, plus three exotic quarks. The latter turn into ordinary quarks with the emission of bilepton doublets (Y^{++}, Y^{+}) and (Y^{--}, Y^{-}) of lepton number $L = -2$ and $L = +2$ respectively, with the doubly-charged bileptons decaying into same-sign lepton pairs. We perform a phenomenological analysis investigating processes with two doubly-charged bileptons and two jets at the LHC and find that, setting suitable cuts on pseudorapidities and transverse momenta of final-states jets and leptons, the model yields a visible signal and the main Standard Model backgrounds can be suppressed. Compared to previous studies, our investigation is based on a full Monte Carlo implementation of the model and accounts for parton showers, hadronization and an actual jet-clustering algorithm for both signal and Standard Model background, thus providing an optimal framework for an actual experimental search.

1. Introduction

The discovery of the Brout–Englert–Higgs (BEH) boson [1,2] has marked a major advance in high-energy physics and neatly completes [3–5] the particle content of the Standard Model (SM) in its current formulation. Through the decades before the confirmation of the BEH (Higgs) mechanism, a wide variety of Beyond the Standard Model (BSM) theories have been advanced [6], usually involving new particles not contained in the SM. The most frequently cited reason for proceeding to BSM from the SM has been the issue of the naturalness of the Higgs mass when quadratic divergences suggest its being much heavier than observed.

The most popular BSM proposal [7,8] has been, for decades, weak-scale supersymmetry; though not being ruled out yet, the LHC data now available regretfully offer no encouragement to supersymmetry. A second popular scenario is based on large extra dimensions, most forcefully extolled in [9], but also with a negative outcome according to current data.

If we abandon the directions of weak scale supersymmetry and large extra dimensions, a more conservative assumption is that the most appropriate BSM theory is a renormalizable gauge field model conceptually identical to the SM but with extra states. One expects the BSM to be motivated by some facts unexplained in the SM and to be testable by experiment. One striking feature of the SM is the existence of three quark–lepton families when the first family alone accounts for the vast majority of the baryonic material while the second and third generations appear at first sight as a curious redundancy. Nevertheless, the family replication is crying out to be a clue. There is an infinite number of possibilities for such a model, selected by the choice of gauge groups and irreducible representations of the chiral fermions, but the requirement of motivation and testability reduce this to a small finite choice.

* Corresponding author.
E-mail addresses: gennaro.corcella@lnf.infn.it (G. Corcella), claudio.coriano@le.infn.it (C. Corianò), antonio.costantini@le.infn.it (A. Costantini), paul.h.frampton@gmail.com (P.H. Frampton).

http://dx.doi.org/10.1016/j.physletb.2017.09.015

The simplest of such models, to our knowledge, is the Bilepton Model[1] of [10,11] where the occurrence of three families is underwritten by cancellation of triangle anomalies.[2] One family, the most massive, is treated asymmetrically[3] and although each family has a non-zero anomaly, the three families combine together to give a vanishing anomaly as essential for consistency.

2. The bilepton model

When the Bilepton Model was introduced, it seemed possible that it was merely one of a large class of such model and therefore had a small probability of being correct. Other than redefinitions of the charge operator, no alternative has been discovered in the intervening 25 years, and therefore it appears more unique than originally thought and thus much more worthy of serious consideration. Here we shall stay with the original formulation [10] with its charge operator which includes *bileptons*, coupled to same-sign leptons.

The model introduces three types of new particles beyond the SM: gauge bosons, exotic quarks and additional scalars. There are five extra gauge bosons which include one Z' and four bileptons in two $SU(2)_L$ doublets (Y^{--}, Y^{-}), with lepton number $L = +2$, as well as (Y^{++}, Y^{+}) with $L = -2$. Each bilepton will decay to two same sign leptons, while exhibiting a coupling to one SM quark and to an exotic quark of the same family, the latter denoted as D, S, and T. The consistency of the model is quite remarkable [13]: we can anticipate that, for the processes which will be investigated in the following, leading to the production of two same-sign lepton pairs and two or more jets, there are about 3000 amplitudes contributing, and the analysis therefore has been automatized. We have implemented the model into `SARAH 4.9.3` [14], with the amplitudes computed numerically using `MadGraph` [15]. The simulation of parton showers and hadronization has been carried out by using `HERWIG` [16].

In this article, our principal focus is on the pair production of these doubly-charged bileptons $Y^{--}Y^{++}$ and their subsequent decay into like-sign lepton pairs, for which we present a detailed simulation of the corresponding events and SM background. As in previous analysis, the Z' of the bilepton model is leptophobic [17] and possesses a decay width comparable to its mass, rendering it an ill-defined resonance with respect to empirical verification. As already mentioned above, four major variants of the model have been discussed recently from the LHC perspective, identified by the value of the charge operator $Q = T^3 + \tilde{\beta} T^8 + X$, with ($\tilde{\beta} = \pm\sqrt{3}, \pm 1/\sqrt{3}$) [18]. We will consider the original model of [10] with $\tilde{\beta} = \sqrt{3}$ which allows doubly-charged bileptons in the spectrum. Notice that only the choices $\pm\sqrt{3}$ allow doubly-charged bileptons. We do not discuss the production and decays of new scalars because those results will be less specific to the model considered in this paper.

3. Theoretical framework

As already stated above, the gauge structure of the bilepton model of [10,11] is $SU(3)_c \times SU(3)_L \times U(1)_X$, with the fermions in the fundamental of $SU(3)_c$ arranged into triplets of $SU(3)_L$. As already pointed out, the three families of quarks are treated asymmetrically with respect to the weak $SU(3)$ ($SU(3)_L$), with the first two families given by

$$Q_1 = \begin{pmatrix} u_L \\ d_L \\ D_L \end{pmatrix}, \quad Q_2 = \begin{pmatrix} c_L \\ s_L \\ S_L \end{pmatrix}, \quad Q_{1,2} \in (3, 3, -1/3) \tag{1}$$

under $SU(3)_c \times SU(3)_L \times U(1)_X$, whereas the third family is

$$Q_3 = \begin{pmatrix} b_L \\ t_L \\ T_L \end{pmatrix}, \quad Q_3 \in (3, \bar{3}, 2/3). \tag{2}$$

D, S and T are exotic (extra) quarks, which in our simulation will be in the TeV (1.1–1.3 TeV) mass range. The right-handed quarks ($\bar{q}$), as in the SM case, are gauge singlet under $SU(3)_L$ and carry a representation content given by

$$(d_R, s_R, b_R) \in (\bar{3}, 1, 1/3) \tag{3}$$

$$(u_R, c_R, t_R) \in (\bar{3}, 1, -2/3) \tag{4}$$

$$(D_R, S_R) \in (\bar{3}, 1, 4/3) \tag{5}$$

$$T_R \in (\bar{3}, 1, -5/3). \tag{6}$$

These states are not sufficient to cancel the $SU(3)_L^3$ anomaly, which requires extra states from the leptonic sector assigned to the $\bar{3}$ representation of the same gauge group. The solution is a democratic arrangement of the three lepton generations into triplets of $SU(3)_L$:

$$l = \begin{pmatrix} l_L \\ \nu_l \\ \bar{l}_R \end{pmatrix}, \quad l \in (1, \bar{3}, 0), \quad l = e,\ \mu,\ \tau. \tag{7}$$

[1] We change name from 331-model because it is necessary to specify not only the gauge group but choices of matter representations and electric charge embedding. We change nomenclature only to avoid confusion.

[2] An important and prescient precursor of the Bilepton Model was made in 1980 [12] in a model where, however, the embedding of electric charge does not accommodate doubly-charged bileptonic gauge bosons.

[3] The difference between the otherwise identical models of [10] and [11] is that in the latter it is the first fermion family which is treated asymmetrically, not the third, a choice which does not allow adequate suppression of flavour-changing neutral currents.

In this way the contribution of Q_1 (+9) and Q_2 (+9) in the 3 of $SU(3)_L$ to the $SU(3)_L^3$ anomaly is balanced by the one coming from Q_3 (−9) and by the three generations of leptons L_i ($(-3)\times 3$) assigned to the $\bar{3}$ representation of $SU(3)_L$. For the $SU(3)_c^3$ anomaly, the cancellation is similar to the SM, with a complete balance between left-handed (3×3) colour triplets and right-handed ($-(3+3+2+1)$) colour anti-triplets, and is henceforth obtained only within the quark sector.

This arrangement of the fermions corresponds to the version of the model proposed in Refs. [10,11]. There are, however, other versions of similar models proposed more recently that differ from the original formulation in some essential aspects. For instance, such variants affect the fermion sector with the addition of extra leptons and extra quarks [19] or the flipping between quarks and leptons [20,21] where all the quark fields are in the same representation of $SU(3)_L$ and the lepton families are in different ones, inverting the structure presented above. The non-universality of the underlying gauge structure is one of the most significant aspects of the model which deserves close attention, especially for its implications on the flavour sector.

The scalars of the model, responsible for the electroweak symmetry breaking, come in three triplets of $SU(3)_L$.

$$\rho = \begin{pmatrix} \rho^{++} \\ \rho^{+} \\ \rho^{0} \end{pmatrix} \in (1,3,1), \quad \eta = \begin{pmatrix} \eta^{+} \\ \eta^{0} \\ \eta^{-} \end{pmatrix} \in (1,3,0), \quad \chi = \begin{pmatrix} \chi^{0} \\ \chi^{-} \\ \chi^{--} \end{pmatrix} \in (1,3,-1). \tag{8}$$

The breaking $SU(3)_L \times U(1)_X \to U(1)_{\rm em}$ is obtained in two steps. The vacuum expectation value (vev) of the neutral component of ρ gives mass to the extra gauge bosons, Z', Y^{++} and Y^{+}, as well as the extra quarks D, S and T. This causes the breaking from $SU(3)_L \times U(1)_X$ to $SU(2)_L \times U(1)_Y$; the usual spontaneous symmetry breaking mechanism from $SU(2)_L \times U(1)_Y$ to $U(1)_{\rm em}$ is then obtained through the vevs of the neutral components. The potential is then given by the expression

$$\begin{aligned} V = {} & m_1\,\rho^*\rho + m_2\,\eta^*\eta + m_3\,\chi^*\chi \\ & + \lambda_1(\rho^*\rho)^2 + \lambda_2(\eta^*\eta)^2 + \lambda_3(\chi^*\chi)^2 \\ & + \lambda_{12}\rho^*\rho\,\eta^*\eta + \lambda_{13}\rho^*\rho\,\chi^*\chi + \lambda_{23}\eta^*\eta\,\chi^*\chi \\ & + \zeta_{12}\rho^*\eta\,\eta^*\rho + \zeta_{13}\rho^*\chi\,\chi^*\rho + \zeta_{23}\eta^*\chi\,\chi^*\eta \\ & + \sqrt{2} f_{\rho\eta\chi}\,\rho\,\eta\,\chi \end{aligned} \tag{9}$$

and the neutral component of each triplet acquires a vev and is expanded as

$$\rho^0 = \frac{1}{\sqrt{2}} v_\rho + \frac{1}{\sqrt{2}} \left(\mathrm{Re}\,\rho^0 + i\,\mathrm{Im}\,\rho^0 \right) \tag{10}$$

$$\eta^0 = \frac{1}{\sqrt{2}} v_\eta + \frac{1}{\sqrt{2}} \left(\mathrm{Re}\,\eta^0 + i\,\mathrm{Im}\,\eta^0 \right) \tag{11}$$

$$\chi^0 = \frac{1}{\sqrt{2}} v_\chi + \frac{1}{\sqrt{2}} \left(\mathrm{Re}\,\chi^0 + i\,\mathrm{Im}\,\chi^0 \right). \tag{12}$$

The minimization conditions of the potential, defined by $\frac{\partial V}{\partial \Phi}|_{\Phi=0} = 0$, then take the form

$$m_1 v_\rho + \lambda_1 v_\rho^3 + \frac{\lambda_{12}}{2} v_\rho v_\eta^2 - f_{\rho\eta\chi} v_\eta v_\chi + \frac{\lambda_{13}}{2} v_\rho v_\chi^2 = 0 \tag{13}$$

$$m_2 v_\eta + \lambda_2 v_\eta^3 + \frac{\lambda_{12}}{2} v_\rho^2 v_\eta - f_{\rho\eta\chi} v_\rho v_\chi + \frac{\lambda_{23}}{2} v_\eta v_\chi^2 = 0 \tag{14}$$

$$m_3 v_\chi + \lambda_3 v_\chi^3 + \frac{\lambda_{13}}{2} v_\rho^2 v_\chi - f_{\rho\eta\chi} v_\rho v_\eta + \frac{\lambda_{23}}{2} v_\eta^2 v_\chi = 0 \tag{15}$$

and are solved for m_1, m_2 and m_3. After spontaneous symmetry breaking the gauge and the mass eigenstates of ρ, η and χ are related by rotation matrices $\mathcal{R}$, whose expressions are rather lengthy to be given here. In the CP-even neutral sector, for instance, the transformation is given by

$$h_i = \mathcal{R}^S_{ij} H_j, \tag{16}$$

where $\vec{H} = (\mathrm{Re}\,\rho^0,\ \mathrm{Re}\,\eta^0,\ \mathrm{Re}\,\chi^0)$ and $\vec{h} = (h_1, h_2, h_3)$. The explicit expression of the mass matrices of the scalar sector, both neutral and charged, can be computed quite directly

$$\mathcal{M}^h = \begin{pmatrix} 2\lambda_1 v_\rho^2 + \frac{f_{\rho\eta\chi}}{v_\rho} V^2 \cos\beta \sin\beta\,, & \lambda_{12} v_\rho V \sin\beta - f_{\rho\eta\chi} V \cos\beta\,, & V(\lambda_{13} v_\rho \cos\beta - f_{\rho\eta\chi} \sin\beta) \\ \lambda_{12} v_\rho V \sin\beta - f_{\rho\eta\chi} V \cos\beta\,, & 2\lambda_2 V^2 \sin^2\beta + f_{\rho\eta\chi} v_\rho \cot\beta\,, & \lambda_{23} V^2 \cos\beta \sin\beta - f_{\rho\eta\chi} v_\rho \\ V(\lambda_{13} v_\rho \cos\beta - f_{\rho\eta\chi} \sin\beta)\,, & \lambda_{23} V^2 \cos\beta \sin\beta - f_{\rho\eta\chi} v_\rho\,, & 2\lambda_3 V^2 \cos^2\beta + f_{\rho\eta\chi} v_\rho \tan\beta \end{pmatrix}, \tag{17}$$

$$\mathcal{M}^a = \begin{pmatrix} \frac{f_{\rho\eta\chi}}{v_\rho} V^2 \cos\beta \sin\beta & f_{\rho\eta\chi} V \cos\beta & f_{\rho\eta\chi} V \sin\beta \\ f_{\rho\eta\chi} V \cos\beta & f_{\rho\eta\chi} v_\rho \cot\beta & f_{\rho\eta\chi} v_\rho \\ f_{\rho\eta\chi} V \sin\beta & f_{\rho\eta\chi} v_\rho & f_{\rho\eta\chi} v_\rho \tan\beta \end{pmatrix}, \tag{18}$$

$$\mathcal{M}^{h^{\pm}} = \begin{pmatrix} \frac{V^2}{2v_\rho}\sin\beta(2f_{\rho\eta\chi}\cos\beta+\zeta_{12}v_\rho\sin\beta) & f_{\rho\eta\chi}V\cos\beta+\frac{1}{2}\zeta_{12}v_\rho V\sin\beta & 0 & 0 \\ f_{\rho\eta\chi}V\cos\beta+\frac{1}{2}\zeta_{12}v_\rho V\sin\beta & \frac{1}{2}v_\rho(\zeta_{12}v_\rho+2f_{\rho\eta\chi}\cot\beta) & 0 & 0 \\ 0 & 0 & \frac{1}{2}\zeta_{23}V^2\cos^2\beta+f_{\rho\eta\chi}v_\rho\cot\beta & \frac{1}{2}\zeta_{23}\cos\beta\sin\beta V^2+f_{\rho\eta\chi}v_\rho \\ 0 & 0 & \frac{1}{2}\zeta_{23}\cos\beta\sin\beta V^2+f_{\rho\eta\chi}v_\rho & \frac{1}{2}\zeta_{23}V^2\sin^2\beta+f_{\rho\eta\chi}v_\rho\tan\beta \end{pmatrix}, \tag{19}$$

$$\mathcal{M}^{h^{\pm\pm}} = \begin{pmatrix} \frac{V^2}{2v_\rho}\cos\beta(\zeta_{13}v_\rho\cos\beta+2f_{\rho\eta\chi}\sin\beta) & \frac{1}{2}\zeta_{13}v_\rho V\cos\beta+f_{\rho\eta\chi}V\sin\beta \\ \frac{1}{2}\zeta_{13}v_\rho V\cos\beta+f_{\rho\eta\chi}V\sin\beta & \frac{1}{2}v_\rho(\zeta_{13}v_\rho+2f_{\rho\eta\chi}\tan\beta) \end{pmatrix}, \tag{20}$$

while their diagonalization has been performed numerically with the parameter choice which will be discussed below. Notice that we have used the definition

$$V=\sqrt{v_\eta^2+v_\chi^2}=246\ \text{GeV}\,,\ \tan\beta=\frac{v_\eta}{v_\chi} \tag{21}$$

for the vevs appearing in the equations above.

4. Phenomenological analysis

In this section we wish to present a phenomenological analysis, displaying possible signals of the bilepton model at the LHC. As discussed in the previous sections, the striking feature of the model is the prediction of doubly-charged gauge bosons Y^{++} and Y^{--} and we shall investigate several physical observables which will be sensitive to the existence of bileptons.

4.1. State of the art of bilepton phenomenology

Before presenting our results, we would like to review several interesting studies which have been so far undertaken and overlap with our analysis [22–27].

Ref. [22] studies single doubly-charged bilepton ($Y^{++,--}$) production in association with exotic quarks D of charge $-4/3$, say $pp\to Y^{++}D$, and possible subsequent decays, such as $D\to Y^{--}q$ or $D\to Y^{-}q'$, q and q' being Standard Model quarks, followed by the leptonic decays of Y^{--} and Y^{-}. The total inclusive cross section was then computed at leading-order (LO), for both bilepton signal and ZZ and $W^{\pm}Z$ backgrounds, at Tevatron and LHC, as a function of Y and exotic-quark masses.

The work in [23] considered instead $Y^{++}Y^{--}$ pairs in Drell–Yan processes, i.e. $pp\to Z,\gamma,Z'\to Y^{++}Y^{--}$, as well as the production of pairs of one doubly- and one singly-charged bilepton, i.e. $Y^{++}Y^{-}(Y^{--}Y^{+})$, mediated by Z, Z', $W^{\pm}$ and photons. The total cross section was computed at LO for different values of Y and Z' masses, for both vector and scalar bileptons. The potential for bilepton discovery at Tevatron and LHC was discussed as well.

Ref. [24] investigated the pair production of singly-charged heavy vectors, which the authors call V, say $pp\to V^{+}V^{-}$, the dependence of the LO cross section on the mediating-Z' mass and its comparison with respect to the $W^{+}W^{-}$-driven Standard Model background.

The analysis in [24] was then extended in [25] with the inclusion of the leptonic decays of singly-charged bileptons and the comparison of few leptonic distributions against the WW background. In [25] the doubly-charged Drell–Yan bilepton production was also accounted for and same-sign dilepton invariant mass and transverse momentum spectra were presented, in terms of Z' and Y masses, at LO matrix-element level; no background was nevertheless computed.

Ref. [26] investigated the production of leptoquarks, labelled as J_3, in pp collisions, through both electroweak (Drell–Yan like) and strong interactions, and possible decays of J_3 into singly- or doubly-charged bileptons, denoted by $V^{\pm}$ and $U^{++,--}$, plus a bottom or a top quark. The total cross sections were calculated at LO and the full process $pp\to J_3J_3\to(Y^{++}Y^{--})(b\bar{b})\to(\ell^{+}\ell^{+})(\ell^{-}\ell^{-})(b\bar{b})$ was then examined; the same-sign $\ell\ell$ and $\ell\ell b$ invariant masses were then studied, varying m_{J_3} and $m_{Z'}$. Once again, the results in [26] were just at matrix-element level, with no parton shower or hadronization matching; the background distributions were not shown, as the authors said that they were negligible with respect to the signal, after applying acceptance cuts on jets (partons) and leptons.

More recently, Ref. [27] explored the LHC potential for discovering bileptons in $pp\to Y^{++}Y^{--}\to\mu^{+}\mu^{+}\mu^{-}\mu^{-}$, with Y-pair production mediated by either a vector boson (γ, Z, Z') or an leptoquark Q. The authors of [27] implemented the bilepton model in the matrix-element generator `CalcHEP` [28], matched with `PYTHIA` [29], and found that the 7 TeV ATLAS data on doubly-charged Higgs production [30], for a luminosity $\mathcal{L}=5$ fb^{-1}, allow one to exclude bileptons between 250 and 500 GeV, depending on the mass of the exotic quarks. Such results were extended to $\sqrt{s}=13$ TeV and $\mathcal{L}=50$ fb^{-1}: by means of a single-bin analysis, based on a Bayesan technique, lower bound $m_{Y^{\pm\pm}}>850$ GeV was obtained.

The analysis which we shall carry out will be concentrated on events with two same-sign lepton pairs and two jets and it should complement the existing studies on bilepton phenomenology. In fact, as discussed above, the work in Refs. [22–27] did cover a large portion of the relevant parameter space for bilepton production at LHC. In particular, Ref. [26], where final states with two jets and two bileptons were explored, determined the LHC reach for bilepton discovery at both 7 and 14 TeV energies, for a wide range of Z' and leptoquark masses.

On the contrary, in the present paper we shall undertake our analysis at 13 TeV and limit ourselves to a benchmark point of the parameter space (mass spectrum), chosen in such a way to enhance the bilepton signal and consistent with the Higgs discovery as well as the present exclusion limits on new particles, such as Y and Z'. Moreover, as done in [27] for jetless YY-pair production, we shall implement our model in the framework of a full Monte Carlo simulation, including parton showers and hadronization. The UFO (Universal FeynRules Output) model generated by `SARAH` will be used by `MadGraph` to generate the relevant amplitudes, which will be matched to `HERWIG` for parton showers and hadronization. Thanks to the implementation of the model in `MadGraph`, the matrix elements for any process, such as $pp\to Y^{++}Y^{--}jj$, will include all the possible subprocesses predicted by the model under investigation.

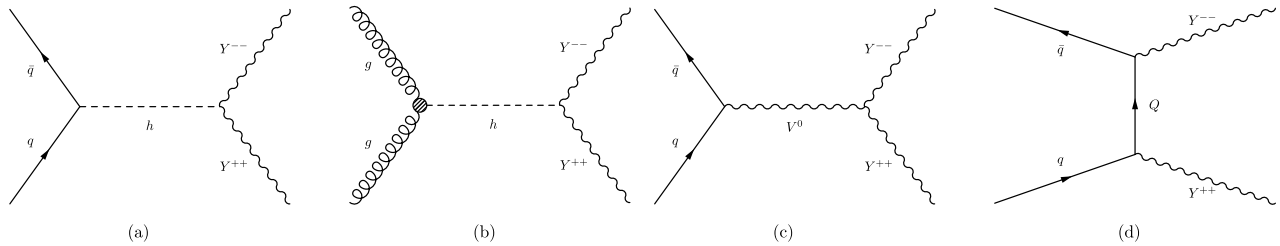

Fig. 1. List of the typical contributions to the events with two bileptons in the final state with no jets.

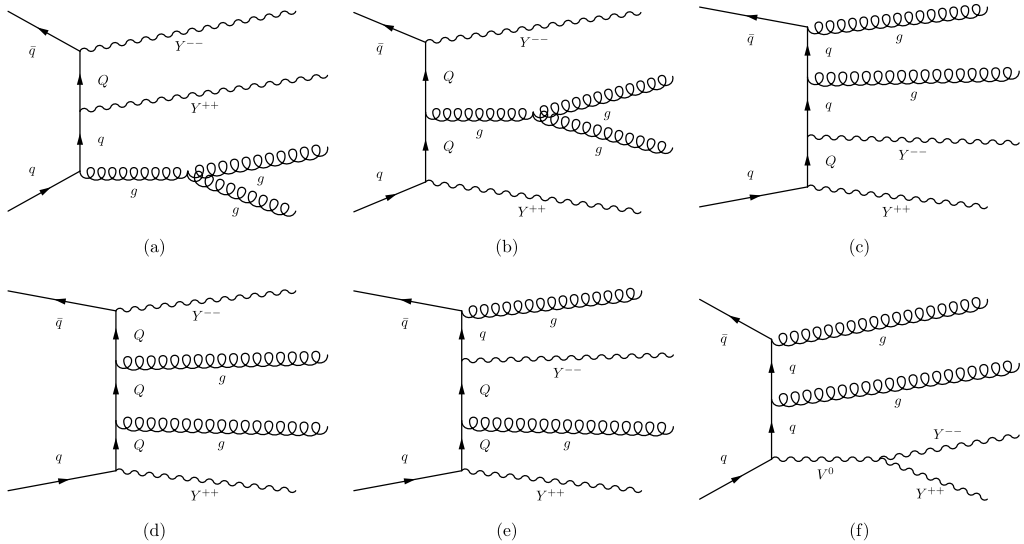

Fig. 2. Typical contributions to the events with two bileptons in the final state at $\mathcal{O}(e^4g^2)$ mediated by one or more exotic intermediate quarks with no extra (W, γ, Z, Z') gauge bosons (diagrams (a)–(e)) and with one extra neutral gauge boson (diagram (f)).

Although the total cross section will still be the LO one, the differential distributions will account for multi-parton radiation and will therefore be equivalent to those yielded by a leading-logarithmic resummed calculation (see, e.g., [31] on the comparison between parton shower algorithms and resummations). The matching of matrix elements and parton showers will also enrich the jet substructure, thus allowing us to implement an actual jet-clustering algorithm: on the contrary, in the work [26], since there was no showering, jets were just identified as partons at the amplitude (`MadGraph`) level. Furthermore, our Monte Carlo event generation has been designed in such a way that it can be directly interfaced to any detector simulation, so that it can be straightforwardly employed by the ATLAS and CMS Collaborations to search for doubly-charged bileptons, extending the current analyses on doubly-charged scalar Higgs bosons [30,32,33].

The same procedure adopted for the bilepton signal will be followed for the Standard Model backgrounds, which will be simulated by `MadGraph` and matched to `HERWIG` for showers and hadronization. Therefore, unlike Refs. [25,26], which did include the background, but only at amplitude-level, even our Standard Model distributions will account for multiple gluon/quark radiation from initial- and final-state partons and jet-clustering algorithm implementation.

Fig. 1 presents typical diagrams wherein bilepton pairs $Y^{++}Y^{--}$ are produced at hadron colliders. Figs. 1 (a) and 1 (c) are Drell–Yan like processes, where h is the SM-like Higgs and V^0 a photon or a Z boson, whereas Fig. 1 (b) refers to bilepton-pair production by gluon fusion, mediated by a h. In Fig. 1 (d) $Y^{++}Y^{--}$ production occurs via the exchange of an exotic quark Q in the t-channel.

In our study we shall nevertheless investigate more exclusive final states, wherein the two same-sign lepton pairs are accompanied by at least two additional jets (jj): Some typical Feynman diagrams contributing to final states with $Y^{++}Y^{--}jj$, where $j = q, g$ at parton level, are depicted in Figs. 2–4. In detail, Fig. 2 includes processes initiated by a $q\bar{q}$ pair and mediated by light or exotic quarks, neutral vector bosons or gluons, but no scalars. Fig. 3 presents characteristic amplitudes where bilepton production occurs through $h \to Y^{++}Y^{--}$ decays in processes with initial-state quarks. Finally, Fig. 4 shows instead some typical diagrams with quark–gluon or gluon–gluon fusion in the initial state. Although the $Z' \to Y^{++}Y^{--}$ subprocess still contributes to $Y^{++}Y^{--}jj$ final states, it is less crucial than in the Drell–Yan processes investigated in [23–25]. We can therefore anticipate that we shall not present results for different Z'-mass values, but we shall stick to one benchmark scenario. Moreover, while the investigation in [26] was based on b-flavoured jets, we shall account for jets of all types, initiated by both light and heavy quarks, as well as by gluons.

4.2. Results at 13 TeV LHC

The phenomenology of our model is very rich due to the structure of both gauge and scalar sectors. For the sake of undertaking an actual LHC analysis, possibly useful for the experimental BSM searches, we have selected a specific benchmark point in parameter space, as given in Table 1 and satisfying a certain number of constraints.

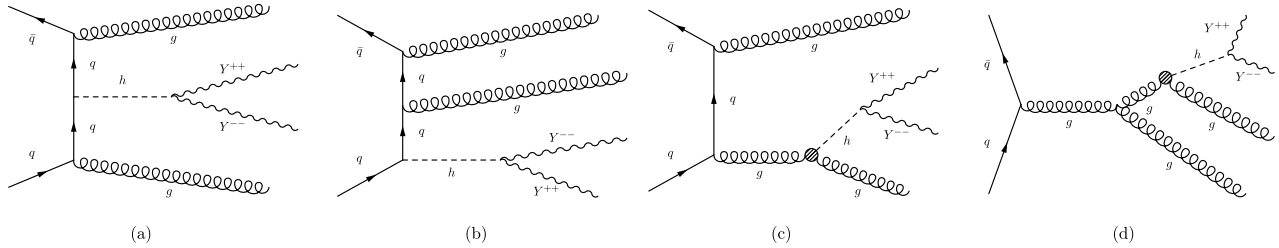

Fig. 3. Processes with two bileptons in the final state at $\mathcal{O}(e^4 g^2)$ with an intermediate Higgs scalar.

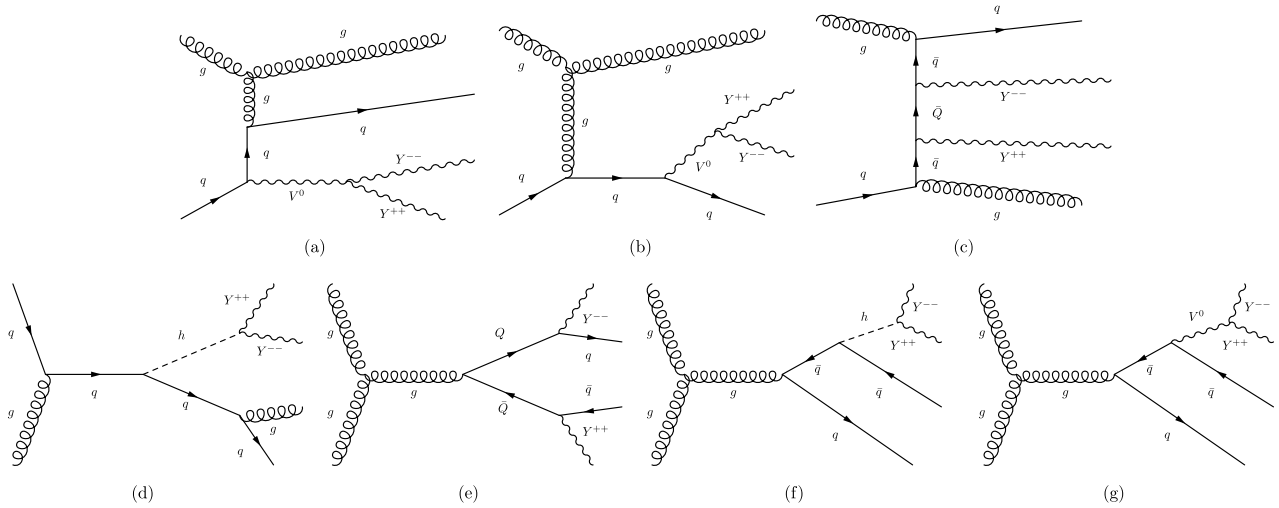

Fig. 4. Bilepton signal from quark–gluon fusion and gluon–gluon fusion.

Table 1
Benchmark point for a collider study consistent with the ~ 125 GeV Higgs mass.

Benchmark Point		
$m_{h_1} = 125.1$ GeV	$m_{h_2} = 3172$ GeV	$m_{h_3} = 3610$ GeV
$m_{a_1} = 3595$ GeV		
$m_{h_1^\pm} = 1857$ GeV	$m_{h_2^\pm} = 3590$ GeV	
$m_{h_1^{\pm\pm}} = 3734$ GeV		
$m_{Y^{\pm\pm}} = 873.3$ GeV	$m_{Y^\pm} = 875.7$ GeV	
$m_{Z'} = 3229$ GeV		
$m_D = 1650$ GeV	$m_S = 1660$ GeV	$m_T = 1700$ GeV

As already explained previously, the vevs of η and χ are responsible for the masses of the known quarks as well as for the masses of the W and Z gauge bosons. Concerning the scalar sector, we require the lightest scalar boson h_1 to be the candidate Higgs boson. Our reference point has therefore been chosen in such a way to yield $m_{h_1} \simeq 125$ GeV. Furthermore, the coupling of h_1 to Z and W has been chosen to be SM-like:

$$\left| \frac{g_{h_1 ZZ}}{g_{hZZ}^{\rm SM}} \right| = 1.0 \pm 0.1 \tag{22}$$

$$\left| \frac{g_{h_1 WW}}{g_{hWW}^{\rm SM}} \right| = 1.0 \pm 0.1. \tag{23}$$

The coupling of the Higgs boson h_1 to top quarks is also SM-like, in such a way that our model reproduces the experimental cross section of Higgs production in gluon fusion, i.e. $gg \to h$.

Beside the SM-like Higgs, we have imposed some other constraints on the new particles of the model. As for bileptons, their mass at tree-level is given by

$$m_{Y^{\pm\pm}} = \frac{1}{2} g_2 \sqrt{v_\rho^2 + V^2 \cos^2 \beta}. \tag{24}$$

In our benchmark point, we have set $m_{Y^{\pm\pm}} \simeq 873$ GeV, while the singly-charged $Y^\pm$ are slightly heavier, i.e. $m_{Y^\pm} \simeq 876$ GeV; such mass values are consistent with the exclusion limits obtained in Ref. [27]. The masses of the extra quarks are related, of course, to their

Yukawa couplings. However, we have chosen m_D, m_S and m_T in such a way that the two-body decay of the extra neutral boson Z' becomes kinematically forbidden, i.e. $m_{Z'} < 2m_Q$. We give in the Appendix the list of the relevant vertices of our model that have been implemented.

In the following, we shall present results for the production of two bileptons plus two jets at the LHC

$$pp \to Y^{++}Y^{--}jj \to (\ell^+\ell^+)(\ell^-\ell^-)jj, \tag{25}$$

where $\ell = e, \mu$. The amplitude of process (25) is generated by the `MadGraph` code, matched with `HERWIG` 6 for shower and hadronization. We have set $\sqrt{s} = 13$ TeV and chosen the NNPDFLO1 parton distributions [34], which are the default sets in `MadGraph`.

We cluster jets at parton level according to the k_T algorithm [35] with $R = 1$, setting the following cuts on jets and lepton transverse momentum (p_T), pseudorapidity (η) and invariant opening angle (ΔR):

$$p_{T,j} > 30 \text{ GeV}, p_{T,\ell} > 20 \text{ GeV}, |\eta_j| < 4.5, |\eta_\ell| < 2.5, \Delta R_{jj} > 0.4, \Delta R_{\ell\ell} > 0.1, \Delta R_{j\ell} > 0.4. \tag{26}$$

After such cuts are applied, the LO cross section, computed by `MadGraph`, reads

$$\sigma(pp \to YYjj \to 4\ell jj) \simeq 3.7 \text{ fb}. \tag{27}$$

As for the background, final states with four charged leptons and two jets may occur through intermediate Z-boson pairs

$$pp \to ZZ\ jj \to (\ell^+\ell^-)(\ell^+\ell^-)jj. \tag{28}$$

We shall also consider processes with intermediate $t\bar{t}Z$ states, with the Z's and the W's from top quarks decaying leptonically, and require a cut MET < 100 GeV on the missing transverse energy carried by the neutrinos

$$pp \to t\bar{t}Z \to (j\ell^+\nu_\ell)(j\ell^-\bar{\nu}_\ell)(\ell^+\ell^-). \tag{29}$$

Obviously, in process (29) the two jets are to be considered b-jets. On the leptons and the jets of both background processes we set the same cuts as in (26). The LO cross sections are then given by

$$\sigma(pp \to ZZ\ jj \to 4\ell jj) \simeq 6.4 \text{ fb}\ ,\ \sigma(pp \to t\bar{t}Z\ jj \to 4\ell\, 2\nu\ jj) \simeq 8.6 \text{ fb}. \tag{30}$$

In principle, within the backgrounds, one should also consider $t\bar{t}h$ processes, with $h \to \ell^+\ell^-$. However, because of the tiny coupling of the Higgs boson to electrons and muons, such a background turns out to be negligible.

Fig. 5 shows the results of our simulation for the signal (solid histograms), as well as ZZ (dashes) and $t\bar{t}Z$ (dots) backgrounds. In detail, we present the spectra of the lepton transverse momentum p_T (a), pseudorapidity η (b), $\ell^\pm\ell^\pm$ invariant mass $m_{\ell\ell}$ (c), angle between same-sign leptons $\theta_{\ell\ell}$ (d), invariant opening angle $\Delta R_{j\ell}$ between the hardest jets and its closest lepton (e), and hardest-jet transverse momentum $p_{T,j1}$ (f). We have plotted everywhere normalized distributions, such as $1/\sigma(d\sigma/dp_T)$, but the normalization of our spectra to the total cross sections computed above is quite straightforward. Moreover, because of the symmetry of our final states, we have included in the histograms all four leptons and we have suitably normalized the distributions.

A general feature of our results is that our bilepton signal can be easily separated from the background. In particular, as for the p_T spectrum, the background distributions are peaked at low p_T and vanish for $p_T > 300$ GeV, while the rate yielded by the bilepton model is substantial up to about 1.3 TeV.

Our results show that the Bilepton Model model predicts a higher event fraction with leptons at central rapidities, say $|\eta| < 1$, and relative angles in the range $1 < \theta_{\ell\ell} < 2$ respect to other kinematical configurations. The invariant mass $m_{\ell\ell}$ distributions are indeed very different. The signal peaks at $m_{Y^{++}} \simeq 873$ GeV and manifests as a narrow resonance, whereas the backgrounds yield broader spectra, peaked around 80 GeV, and roughly vanishing for $m_{\ell\ell} > 350$ GeV. The $\Delta R_{j\ell}$ and p_{tj1} spectra are less different than the others, but nevertheless there is a visible discrepancy at low $\Delta R_{j\ell}$ and p_{tj1}.

5. Discussion

The most popular BSM models, supersymmetry and large extra dimensions, although not yet excluded, have received no encouragement from the late LHC data, since no new particle has so far been discovered.

A more conservative approach is the model of [10], whose phenomenology has been examined in this paper. Of the new particles of the model, the bilepton gauge bosons have striking signatures at the LHC. As clear from Fig. 5, the large transverse-momentum rate sets the clearest distinction of this model respect to the SM. Specifically, by imposing a cut in p_T enforcing a large transverse momentum above 300 GeV, or even $p_T > 500$ GeV, the SM background can be successfully suppressed to the extent that the bilepton signal, if it is present, cannot be missed in the experimental analysis.

Another hint in this direction, also evident from Fig. 5, is to focus on the central region with pseudorapidity $|\eta| < 1$ or relative angle $1 < \theta_{\ell\ell} < 2$, which further enhances the rates for this model with respect to the SM ones. The reason is physically clear when one realizes that the massive bileptons are produced with rather low momenta in the centre-of mass frame, which imply central pseudorapidities in the laboratory frame and larger angles between same-sign leptons. Assuming that the four leptons, accompanied by two jets, are muons, then the invariant mass of di-muon pairs, with the three different permutational combinations (12), (13), (14), can be analyzed as in Fig. 5 to discover decisively the existence of such bilepton particles. With the magnetic fields available at LHC, namely 4 Tesla at CMS and 2 Tesla at ATLAS, the stiff muons may still reveal their electric charges, so that the checking of all three permutations may be obviated.

We therefore believe that searching for bileptons is interesting and quite feasible at the LHC. Our investigation can therefore be seen as a useful starting point to carry out an experimental analysis on the Bilepton Model [10] and its phenomenology, as we have undertaken a full Monte Carlo implementation of both signal and background, including parton shower and hadronization, which allows a straightforward application to the experimental searches. We hope to return in the future with further investigations which may guide and motivate further analyses.

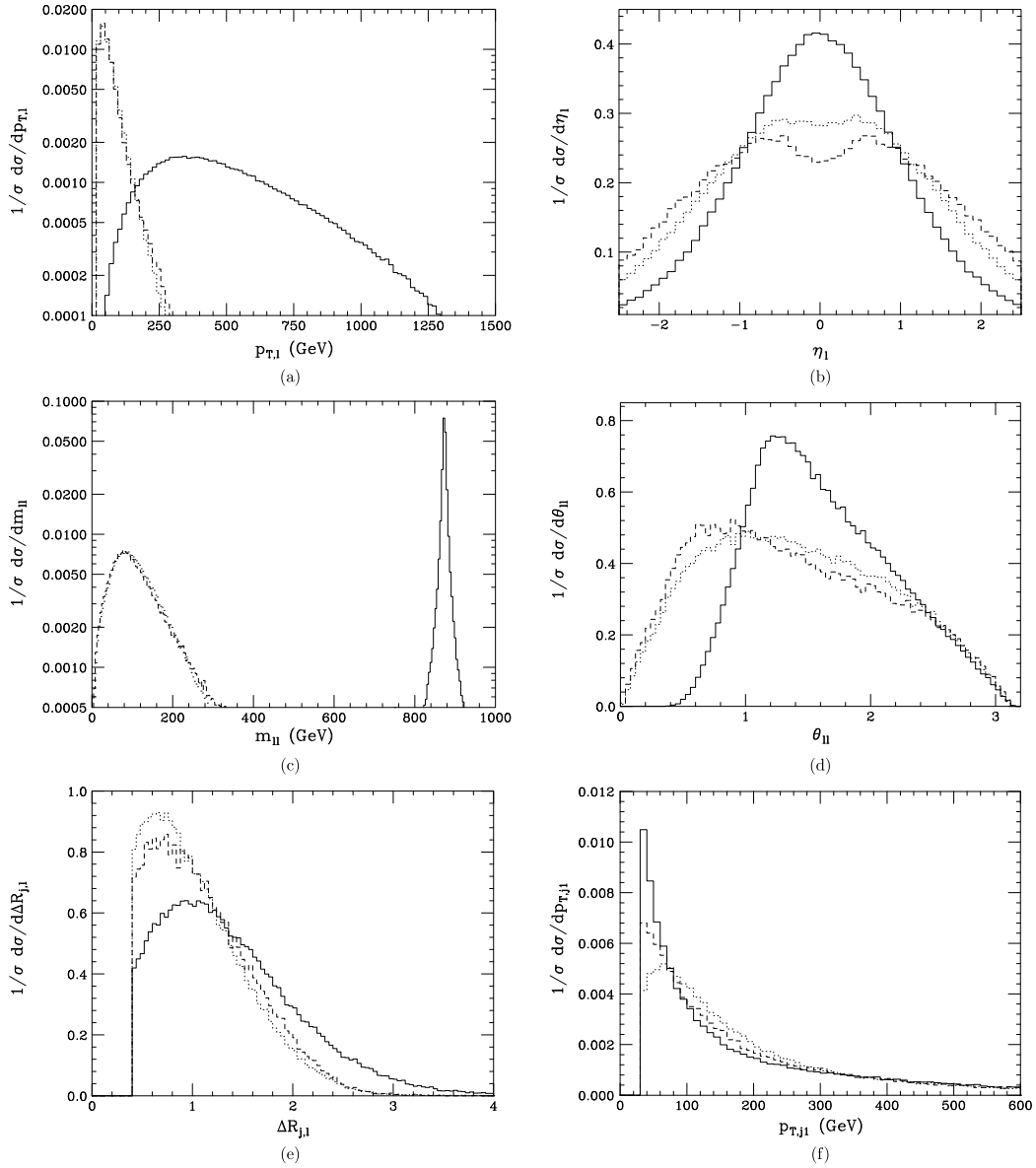

Fig. 5. Results of the simulation: (a) Lepton transverse momentum distribution; (b) Lepton pseudorapidity distribution, (c) Same-sign lepton-pair invariant mass; (d) Angle between same-sign leptons; (e) Invariant opening angle $\Delta R_{j\ell}$ between the hardest jet and its closest lepton; and (f) p_T of the hardest jet j_1. The solid histograms are the bilepton signals, the dashes correspond to the ZZ background, the dots to $t\bar{t}Z$ processes.

Acknowledgements

We acknowledge discussions with Marco Zaro on the use of the `MadGraph` generator and with Gabriele Chiodini, Stefania Spagnolo and Konstantinos Bachas on the experimental applications of our analysis. PHF thanks the INFN and the Department of Physics at the University of Salento for hospitality. C.C. thanks Rhorry Gauld for discussions. The work of C.C. is partially supported by INFN 'Iniziativa Specifica' QFT-HEP.

Appendix A. Vertices

We give the relevant vertices for the bileptons.

$$\ell\,\ell\,Y^{++} = \begin{cases} -\frac{i}{\sqrt{2}} g_2 \gamma^\mu & P_L \\ \frac{i}{\sqrt{2}} g_2 \gamma^\mu & P_R \end{cases} \tag{A.1}$$

$$\bar{d}\, T\, Y^{--} = \begin{cases} -\frac{i}{\sqrt{2}} g_2 \gamma^\mu & P_L \\ 0 & P_R \end{cases} \tag{A.2}$$

$$\bar{D}\, u\, Y^{--} = \begin{cases} \frac{i}{\sqrt{2}} g_2 \gamma^\mu & P_L \\ 0 & P_R \end{cases} \tag{A.3}$$

$$h_i\, Y^{++} Y^{--} = \frac{i}{2} g_2^2 \left(v_\rho \mathcal{R}^S_{i1} + v_\chi \mathcal{R}^S_{i3} \right) \tag{A.4}$$

$$\gamma\, Y^{++} Y^{--} = -2i\, g_2\, \sin\theta_W \tag{A.5}$$

$$Z\, Y^{++} Y^{--} = \frac{i}{2}\, g_2\, (1 - 2\cos 2\theta_W)\, \sec\theta_W \tag{A.6}$$

$$Z'\, Y^{++} Y^{--} = -\frac{i}{2}\, g_2\, \sqrt{12 - 9\sec^2\theta_W}\,. \tag{A.7}$$

References

[1] S. Chatrchyan, et al., CMS Collaboration, Observation of a new boson at a mass 125 GeV with the CMS experiment at the LHC, Phys. Lett. B 716 (2012) 30, arXiv:1207.7235 [hep-ex].
[2] G. Aad, et al., ATLAS Collaboration, Observation of a new particle in the search for the Standard Model Higgs boson with the ATLAS detector at the LHC, Phys. Lett. B 716 (2012) 1, arXiv:1207.7214 [hep-ex].
[3] P.W. Higgs, Broken symmetries, massless particles and gauge fields, Phys. Lett. 12 (1964) 132.
[4] P.W. Higgs, Broken symmetries and masses of gauge bosons, Phys. Rev. Lett. 13 (1964) 321.
[5] R. Brout, F. Englert, Broken symmetry and mass of gauge vector mesons, Phys. Rev. Lett. 13 (1964) 321.
[6] P. Horava, Surprises with nonrelativistic naturalness, Int. J. Mod. Phys. D 25 (2016) 1645007.
[7] J. Wess, B. Zumino, A Lagrangian model invariant under supergauge transformations, Phys. Lett. B 49 (1974) 52.
[8] J. Wess, B. Zumino, Supergauge transformations in four dimensions, Nucl. Phys. B 70 (1974) 39.
[9] N. Arkani-Hamed, S. Dimopoulos, G.R. Dvali, The hierarchy problem and new dimensions at a millimeter, Phys. Lett. B 429 (1998) 263, arXiv:hep-ph/9803315.
[10] P.H. Frampton, Chiral dilepton model and the flavor question, Phys. Rev. Lett. 69 (1992) 2889.
[11] F. Pisano, V. Pleitez, An SU(3) x U(1) model of electroweak interactions, Phys. Rev. D 46 (1992) 410.
[12] M. Singer, J.W.F. Valle, J. Schechter, Canonical neutral current predictions from the weak electromagnetic group $SU(3) \times U(1)$, Phys. Rev. D 22 (1980) 738.
[13] B. Meirose, A.A. Nepomuceno, Searching for doubly-charged vector bileptons in the golden channel at the LHC, Phys. Rev. D 84 (2011) 055002, arXiv:1105.6299 [hep-ph].
[14] F. Staub, SARAH 4: a tool for (not only SUSY) model builders, Comput. Phys. Commun. 185 (2014) 1773, arXiv:1309.7223 [hep-ph].
[15] J. Alwall, et al., The automated computation of tree-level and next-to-leading order differential cross sections, and their matching to parton shower simulations, J. High Energy Phys. 1407 (2014) 07, arXiv:1405.0301 [hep-ph].
[16] G. Corcella, et al., HERWIG 6: an event generator for hadron emission reactions with interfering gluons (including supersymmetric processes), J. High Energy Phys. 0101 (2001) 010, arXiv:hep-ph/0011363.
[17] D. Gomez Dumm, Leptophobic character of the Z-prime in an $SU(3)_C \times SU(3)_L \times U(1)_X$ model, Phys. Lett. B 411 (1997) 313, arXiv:hep-ph/9709245.
[18] Q.H. Cao, D.M. Zhang, Collider phenomenology of the 3–3–1 model, arXiv:1611.09337 [hep-ph].
[19] A.J. Buras, F. De Fazio, J. Girrbach, M.V. Carlucci, The anatomy of quark flavour observables in 331 models in the flavour precision era, J. High Energy Phys. 1302 (2013) 023, arXiv:1211.1237 [hep-ph].
[20] R. Gauld, F. Goertz, U. Haisch, An explicit Z'-boson explanation of the $B \to K^* \mu^+ \mu^-$ anomaly, J. High Energy Phys. 1401 (2014) 069, arXiv:1310.1082 [hep-ph].
[21] R.M. Fonseca, M. Hirsch, A flipped 331 model, J. High Energy Phys. 1608 (2016) 003, arXiv:1606.01109 [hep-ph].
[22] B. Dutta, S. Nandi, Search for dilepton gauge bosons in hadron colliders, Phys. Lett. B 340 (1994) 86.
[23] B. Dion, T. Grégoire, D. London, L. Marleau, H. Nadeau, Bilepton production at hadron colliders, Phys. Rev. D 59 (1999) 075006, arXiv:hep-ph/9810534.
[24] E.R. Barreto, Y.A. Coutinho, J. Sá Borges, Charged bilepton pair production at LHC including exotic quark contribution, Nucl. Phys. B 810 (2009) 210, arXiv:0811.0846 [hep-ph].
[25] E.R. Barreto, Y.A. Coutinho, J. Sá Borges, Vector-bilepton contribution to four lepton production at the LHC, Phys. Rev. D 88 (2013) 035016, arXiv:1307.4683 [hep-ph].
[26] A. Alves, E. Ramirez Barreto, A.G. Dias, Jets plus same-sign dileptons signatures from fermionic leptoquarks, Phys. Rev. D 86 (2012) 055025, arXiv:1203.3242 [hep-ph].
[27] A.A. Nepumuceno, F.L. Eccard, B. Meirose, First results on bilepton production based on LHC collision data and predictions for run II, Phys. Rev. D 94 (2016) 055020.
[28] A. Belyaev, N. Christensen, A. Pukhov, CalcHEP 3.4 for collider physics within and beyond the Standard Model, Comput. Phys. Commun. 184 (2013) 1729.
[29] T. Sjöstrand, S. Mrenna, P. Skands, A brief introduction to PYTHIA 8.1, Comput. Phys. Commun. 178 (2008) 852.
[30] ATLAS Collaboration, Search for doubly-charged Higgs bosons in like-sign dilepton final states at $\sqrt{s} = 7$ TeV with the ATLAS detector, Eur. Phys. J. C 72 (2012) 2244.
[31] S. Catani, G. Marchesini, B.R. Webber, QCD coherent branching and semiinclusive processes at large x, Nucl. Phys. B 349 (1991) 635.
[32] ATLAS Collaboration, Search for doubly-charged Higgs boson production in multi-lepton final states with the ATLAS detector using proton–proton collisions at $\sqrt{s} =$ 13 TeV, ATLAS-CONF-2017-053.
[33] CMS Collaboration, A search for doubly-charged Higgs boson production in three and four lepton final states at $\sqrt{s} = 13$ TeV, CMS-PAS-HIG-16-036.
[34] R.D. Ball, et al., NNPDF Collaboration, Parton distributions with QED corrections, Nucl. Phys. B 877 (2013) 290, arXiv:1308.0598 [hep-ph].
[35] S. Catani, Yu.L. Dokshitzer, M.H. Seymour, B.R. Webber, Longitudinally invariant K_t clustering algorithms for hadron–hadron collisions, Nucl. Phys. B 406 (1993) 187.